

# Template Removal from SBA-15 by Ionic Liquid for Amine Grafting: Applications to CO<sub>2</sub> Capture and Natural Gas Desulfurization

Yiren Wang and Ralph T. Yang\*



Cite This: *ACS Sustainable Chem. Eng.* 2020, 8, 8295–8304



Read Online

ACCESS |

Metrics & More

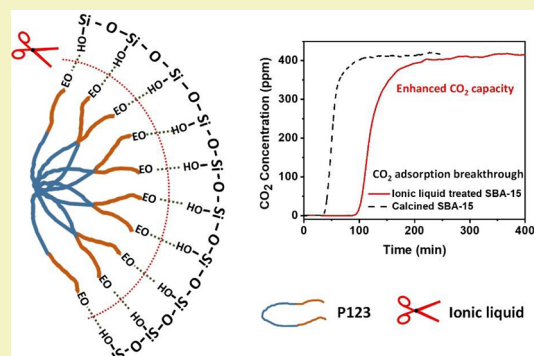
Article Recommendations

Supporting Information

**ABSTRACT:** A new ionic liquid treatment method has been developed for removing the organic template from mesoporous silica SBA-15. Compared with conventional template removal by air calcination, the novel ionic liquid treatment method efficiently removed the organic template at a low temperature and preserved the surface silanol groups. The significantly increased silanol density led to higher amine loadings on amine grafted SBA-15. Consequently, the ionic liquid treated sample showed 63% more CO<sub>2</sub> capacity at conditions relevant to CO<sub>2</sub> capture from flue gas. Moreover, the ionic liquid treated sample exhibited significantly higher capacities for H<sub>2</sub>S capture from natural gas as well as CO<sub>2</sub> adsorption capacities for direct air capture which were nearly 3 times higher than the conventionally treated sample. The adsorbent stability, the isosteric heats of adsorption, and the effect of moisture were also investigated for the ionic liquid treated sample.

The mechanism of template removal by ionic liquid is discussed, and the feasibility of recovery/reuse of the ionic liquid and the template is shown.

**KEYWORDS:** Mesoporous silica SBA-15, Template removal, Ionic liquids, CO<sub>2</sub> capture, H<sub>2</sub>S removal



## INTRODUCTION

Postcombustion carbon dioxide (CO<sub>2</sub>) capture from flue gas and the removal of hydrogen sulfide (H<sub>2</sub>S) from natural gas are important industrial processes. Gas–liquid absorption and stripping processes using aqueous solutions of alkanolamines (monoethanolamine (MEA), diethanolamine (DEA), and methyldiethanolamine (MDEA)) are the bases for the current technologies for postcombustion CO<sub>2</sub> capture and natural gas desulfurization. The liquid amine absorption process, while effective, is plagued by a myriad of problems including high energy consumption during regeneration, corrosion from amine solutions, and amine loss. Therefore, considerable efforts over the past few years have been committed to the development of alternatives.

One such alternative is gas adsorption using solid adsorbents such as carbons,<sup>1–4</sup> zeolites,<sup>5–9</sup> metal–organic frameworks,<sup>10–12</sup> nitrogen-functionalized porous polymers,<sup>13–16</sup> and amine-functionalized silicas.<sup>17–23</sup> The combination of selective capture and catalytic conversion is also an alternative route for CO<sub>2</sub> and H<sub>2</sub>S removal.<sup>24,25</sup> Among all the adsorbents, amine grafted silicas are some of the most promising because of their high capacities, high CO<sub>2</sub> (and H<sub>2</sub>S) selectivities, high adsorption rates, ease in regeneration and low moisture sensitivities.<sup>26</sup> Ordered mesoporous silicas (Mobil Composition of Matter-*n* or MCM-*n*,<sup>27</sup> Santa Barbara Amorphous-*n* or SBA-*n*,<sup>28,29</sup> and hexagonal mesoporous silica or HMS<sup>30</sup>) are of great interest due to their adjustable pore sizes, large surface

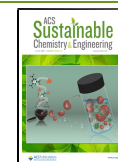
areas, and, most notably, the hydroxyl groups or silanols that dominate the surface. This makes them ideal for postsynthesis amine grafting. Amine grafting is accomplished by a reaction between the surface hydroxyl groups (silanols) of silicas and aminosilanes such as 3-aminotrimethoxysilane. Therefore, increasing silanol density is a facile and effective way of increasing amine group density, which, in turn, leads to an increase in CO<sub>2</sub> (and H<sub>2</sub>S) adsorption capacity on the amine grafted silicas.

Ordered mesoporous silicas are generally obtained by hydrothermal synthesis using organic templates as a structure directing agents, followed by polymerization of the silica precursors around the template. Once this mesoporous structure is formed, the key step in the synthesis process is the removal of the organic template because it creates the desired porosity. The conventional method for template removal is by air calcination at high temperatures (>500 °C) and long treatment time (>4 h). However, calcination at high temperatures result in the reduction of silanol groups due to dehydroxylation at high temperature and long heating time.

Received: March 10, 2020

Revised: April 13, 2020

Published: May 14, 2020



Thus, alternative methods for template removal under mild conditions were developed. Ethanol extraction,<sup>22</sup> glow discharge plasma degradation,<sup>23</sup> UV/dilute H<sub>2</sub>O<sub>2</sub> degradation,<sup>31</sup> supercritical fluid extraction,<sup>32</sup> and microwave digestion<sup>33</sup> have been successfully employed to remove templates from ordered mesoporous silicas. Since the amine grafting reaction is based on silanol groups as the anchor sites, more efforts are desirable for developing effective template removal method at lower temperature and shorter time to preserve as many silanol groups as possible, especially methods that can also preserve and recover the costly organic templates.

Ionic liquid is a salt in which the ions are poorly coordinated, which results in these salts being liquid below 100 °C. Ionic liquids are described as having many potential applications. They are powerful solvents and electrically conducting fluids. Rogers et al. reported that cellulose could be dissolved using ionic liquids, such as 1-butyl-3-methylimidazolium chloride ([C<sub>4</sub>mim]Cl), by breaking the hydrogen bonds within the cellulose.<sup>34,35</sup> Various ionic liquids are effective for lignocellulosic biomass dissolution. A comprehensive and updated review on treatments of lignocellulosic biomass with ionic liquids is available.<sup>36</sup> Brennecke et al. employed ionic liquids with amine groups for CO<sub>2</sub> capture. By the design of anion in ionic liquids, the CO<sub>2</sub> absorption capacities and regeneration energies could be adjusted.<sup>37,38</sup> Deep eutectic solvents, a new class of ionic liquid analogue, are promising media for gas separation.<sup>39</sup> Moreover, ionic liquid can be added to amine-impregnated adsorbents to increase CO<sub>2</sub> adsorption capacity.<sup>40</sup> As designer solvents, ionic liquid can be modulated to suit specific tasks.<sup>41,42</sup>

In this study, we employed a novel ionic liquid treatment as well as the conventional thermal calcination to remove the triblock copolymer template Pluronic P123 from as-synthesized SBA-15. The physical properties, silanol and amine density, and the CO<sub>2</sub> and H<sub>2</sub>S adsorption capacities of SBA-15 utilizing both template removal methods were compared. The mechanism for template removal using ionic liquid was also proposed. To the best of our knowledge, this is the first time ionic liquid is used for SBA-15 template removal.

## EXPERIMENTAL SECTION

**Synthesis of SBA-15.** Mesoporous silica SBA-15 was synthesized using the procedures reported by Zhao et al.<sup>29</sup> using triblock copolymer Pluronic P123 (EO<sub>20</sub>PO<sub>70</sub>EO<sub>20</sub>) as template. Typically, 8 g of Pluronic P123 was added to 240 g of deionized water (DI water) and 48 g of concentrated HCl (37 wt %) at 35 °C and stirred until dissolved. Next, 17 g of TEOS (tetraethyl orthosilicate) was added to the solution. Then the mixture was stirred at 35 °C for 24 h, followed by another 24 h at 100 °C. The solid product (as-synthesized SBA-15) was filtered, washed with DI water, and dried at 50 °C.

**Removal of Template (P123) from As-Synthesized SBA-15.** The ionic liquid 1-butyl-3-methylimidazolium chloride ([C<sub>4</sub>mim]Cl) used to remove template P123 from as-synthesized SBA-15 was purchased from ACROS Organics. In the template removal process by ionic liquid, 1 g of the as-synthesized SBA-15 was mixed with 9 g of [C<sub>4</sub>mim]Cl and then transferred to a Teflon-lined autoclave. The mixture was treated in an oven at 120 °C for 12 h under static conditions. After template removal treatment, the product was washed with DI water, recovered by centrifugation, and then dried at 50 °C. The SBA-15 obtained was designated as SBA-15-IL.

In comparison, the template P123 of as-synthesized SBA-15 was also removed by conventional calcination under air flow at 500 °C for 6 h. The SBA-15 sample obtained from calcination was designated as SBA-15-cal.

**Grafting Amine on SBA-15.** The grafting of amine on SBA-15 surfaces followed the procedures reported in the literature.<sup>22,23</sup> Typically, 0.5 g of SBA-15-cal or SBA-15-IL was mixed with 50 mL of toluene and 5 mL of 3-aminopropyltrimethoxysilane. The mixture was stirred at 80 °C for 18 h under reflux. The resulting product was filtered and washed with a copious amount of toluene and then dried at 50 °C. The obtained samples were designated as NH<sub>2</sub>-SBA-15-cal and NH<sub>2</sub>-SBA-15-IL.

**Adsorption Measurement.** Adsorption isotherms of carbon dioxide, nitrogen, and methane within the pressure range from 0 to 760 Torr were measured with a Micromeritics ASAP 2020 Analyzer, which is a static volumetric apparatus. The hydrogen sulfide adsorption isotherms were measured using a Shimadzu TGA-50H thermogravimetric analyzer, which is a gravimetric method. Quartz sample cells and purge gas (helium) were used for H<sub>2</sub>S isotherm measurement. The adsorbent was pretreated in predried helium at 105 °C for 4 h before the H<sub>2</sub>S isotherm measurement to remove the adsorbed moisture and impurities on the surface. Low concentration H<sub>2</sub>S was obtained by blending predried H<sub>2</sub>S (200 ppm in helium) with predried helium. The total flow rate was 80 mL/min, and the concentration range of H<sub>2</sub>S was 0–125 ppm.

The CO<sub>2</sub> breakthrough curves were measured with a vertical fixed bed equipped with a Vaisala GMP343 CO<sub>2</sub> probe. The Vaisala GMP343 incorporates a silicon-based nondispersive infrared sensor with a measurement range of 0–1000 ppm CO<sub>2</sub>. The procedures for preparing the adsorbent bed were described elsewhere.<sup>43</sup> A slurry made from the amine grafted powder adsorbent and toluene was injected into a Pyrex tube. An indent and a small piece of quartz wool were used to hold the adsorbent bed. The slurry was dried under 60 °C in an air stream flowing at 20 mL/min. For a typical experiment, the fixed bed was set at 4 cm in height and 0.35 cm diameter. Before the adsorption process, the fixed bed column was pretreated at 105 °C for 3 h under nitrogen flow prior to adsorption measurements. The temperature was then reduced to 25 °C and the feed gas (ambient air, predried with a bed of 3A zeolite) was introduced at a gas hourly space velocity (GHSV) of 4200 h<sup>-1</sup>. For the adsorption measurement under wet conditions, the feed stream was passed through a bubbler containing a saturated KCl solution at 25 °C before being introduced to the adsorbent bed.<sup>44</sup>

Multicycle stability studies were examined using a Shimadzu TGA-50H thermogravimetric analyzer under a CO<sub>2</sub> flow (70% in He) of 80 mL/min at 25 °C. The sample was pretreated at 90 °C for 60 min before the first adsorption cycle and desorbed at 90 °C in helium for 10–15 min after each adsorption cycle.

**Characterization.** N<sub>2</sub> adsorption/desorption isotherms at –196 °C were acquired using a Micromeritics ASAP 2020 Analyzer, which is a static volumetric gas adsorption apparatus. The samples were degassed at 105 °C for 6 h before analysis. Thermogravimetric analysis (TGA) was performed on a Shimadzu TGA-50H apparatus to analyze the percentage of template removal, silanol density, and amine loading of the samples. The template removed samples (SBA-15-cal and SBA-15-IL) were heated from room temperature to 850 °C at a heating rate of 5 °C/min under a helium flow for evaluating the percentage of template removal and silanol density. The amine grafted samples NH<sub>2</sub>-SBA-15-cal and NH<sub>2</sub>-SBA-15-IL were heated under helium and air flow to investigate the amine loading. The samples were pretreated at 120 °C in the helium flow to remove adsorbed CO<sub>2</sub> and moisture, and then they were kept at 100 °C in a helium flow for 30 min before being heated to 850 °C at a heating rate of 5 °C/min in an air flow. The NMR spectra were recorded on a Varian vnmrs 500 MHz spectrometer at 25 °C using deuterated chloroform (CDCl<sub>3</sub>) as solvent. Chemical shifts were referenced to TMS (0.0 ppm). A total of 128 scans were collected.

## RESULTS AND DISCUSSION

**Template Removal by Ionic Liquid.** The N<sub>2</sub> adsorption–desorption isotherms of calcined SBA-15 sample (SBA-15-cal) and ionic liquid treated SBA-15 sample (SBA-15-IL) are shown in Figure 1a. Both isotherms exhibited type IV(a)

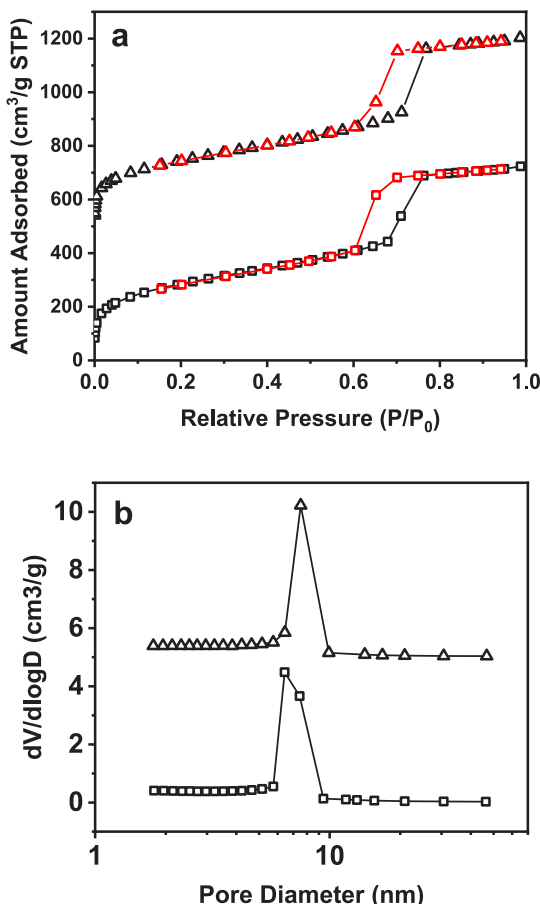


**Figure 1.** N<sub>2</sub> adsorption and desorption isotherms and BJH pore size distribution of SBA-15-cal (□) and SBA-15-IL (△) at  $-196\text{ }^{\circ}\text{C}$ . Isotherms for SBA-15-IL and BJH pore size distributions were offset by  $500\text{ cm}^3/\text{g}$  STP and  $5\text{ cm}^3/\text{g}$  for clarity.

behavior with a type H1 hysteresis loop, according to IUPAC classification.<sup>45</sup> The uptake in the  $P/P_0$  range of 0.6–0.8 corresponds to capillary condensation of nitrogen in the mesopores of SBA-15, and the type H1 loop indicates a narrow range of uniform mesopores. These results are characteristic of good quality SBA-15 and similar to those reported previously.<sup>22,29</sup> The Brunauer–Emmett–Teller (BET) surface area and total pore volume of SBA-15-IL were  $883.5\text{ m}^2/\text{g}$  and  $1.09\text{ cm}^3/\text{g}$ , respectively (Table 1), which are similar to those of SBA-15-cal ( $981.8\text{ m}^2/\text{g}$  and  $1.12\text{ cm}^3/\text{g}$ ). This illustrates that ionic liquid treatment is an effective method of template removal. Figure 1b shows the Barrett–Joyner–Halenda (BJH)

**Table 1. Textual and Structure Parameters of SBA-15 and Amine-Grafted SBA-15 by Thermal Calcination and Ionic Liquid Treatment**

sample	$S_{\text{BET}}^a$ ( $\text{m}^2/\text{g}$ )	$V_{\text{total}}^b$ ( $\text{cm}^3/\text{g}$ )	pore diam <sup>c</sup> (nm)	silanol no. (OH/nm <sup>2</sup> )	estd amine loadings (mmol/g)
SBA-15-cal	981.8	1.12	6.4	3.0	
SBA-15-IL	883.5	1.09	7.5	>5.1	
NH <sub>2</sub> -SBA-15-cal	326.0	0.47	5.6		1.4
NH <sub>2</sub> -SBA-15-IL	239.7	0.38	5.7		2.2

<sup>a</sup>BET surface area calculated from the adsorption branch. <sup>b</sup>Pore volume estimated from the single-point amount adsorbed at  $P/P_0 = 0.95$ . <sup>c</sup>Pore diameter determined by BJH method.

pore size distributions of SBA-15-cal and SBA-15-IL. The BJH pore size distributions were centered at 6.4 nm for SBA-15-cal and 7.5 nm for SBA-15-IL, indicating reduced shrinkage of the mesoporous framework structure via template removal by ionic liquid treatment.

The efficiency of template removal by ionic liquid treatment can be demonstrated by thermogravimetric analysis (TGA). The TGA thermograms of SBA-15-cal and SBA-15-IL are shown in Figure 2. Two major weight loss steps can be

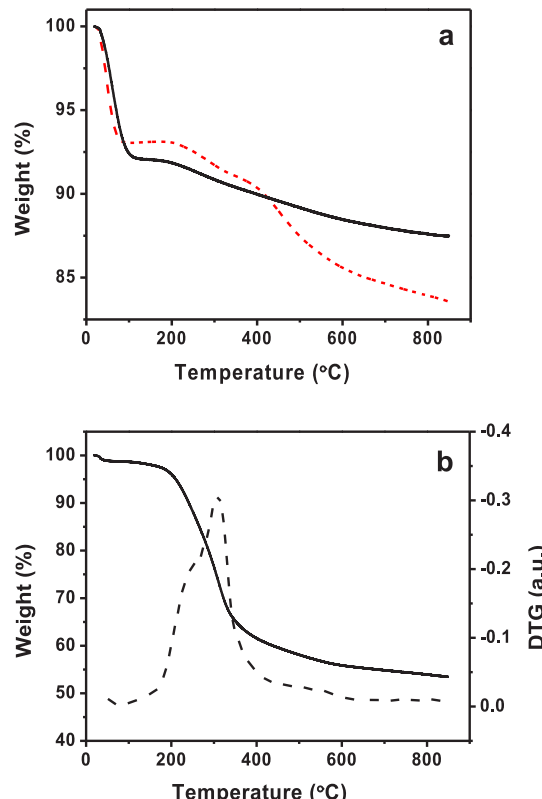


**Figure 2.** (a) TGA thermograms of SBA-15-cal (solid line) and SBA-15-IL (dashed line) in a helium flow. (b) TGA thermogram (solid line) and DTG curve (dashed line) of as-synthesized SBA-15 in a helium flow.

observed for these samples. The weight loss below  $150\text{ }^{\circ}\text{C}$  can be attributed to the removal of physically adsorbed water and other small molecules (i.e., CO<sub>2</sub>). The weight loss from  $150$  to  $850\text{ }^{\circ}\text{C}$  corresponds to the release of water formed during the condensation of silanol groups in the silica framework and the decomposition of organic templates. The percentage of template in as-synthesized SBA-15 was 45.2%, and all of the decomposition occurred between  $200$  and  $400\text{ }^{\circ}\text{C}$  (Figure 2b). As shown in Figure 2a, the weight losses from  $150$  to  $850\text{ }^{\circ}\text{C}$  of SBA-15-cal and SBA-15-IL were 4.5 and 9.5%, respectively. Calcination in air is an effective way to remove template. Therefore, the 4.5% weight loss of SBA-15-cal can be attributed to the condensation of silanol groups. For the case of SBA-15-IL, there are three stages of weight loss: the weight loss below  $150\text{ }^{\circ}\text{C}$ , the weight loss between  $150$  and  $400\text{ }^{\circ}\text{C}$ , and the weight loss above  $400\text{ }^{\circ}\text{C}$ . The weight loss between  $150$  and  $400\text{ }^{\circ}\text{C}$  can be attributed to the combination of remained template decomposition and dehydroxylation of silanol groups. The weight loss above  $400\text{ }^{\circ}\text{C}$  is the condensation of the rest of the silanol groups in SBA-15-IL.

According to the TGA results, the percentage of template removal of SBA-15-IL is at least 92%, indicating the effectiveness of the ionic liquid treatment. Based on the BET surface area, the silanol number of SBA-15-IL was at least 5.1 OH nm<sup>-2</sup>, which was higher than 3.0 OH nm<sup>-2</sup> for SBA-15-cal. These results demonstrate ionic liquid treatment is able to remove template under mild temperature conditions and retain more silanol groups in SBA-15 framework than the thermal calcination.

**Amine Grafted SBA-15 by Ionic Liquid Treatment for Template Removal.** Figure 3 shows the N<sub>2</sub> adsorption–

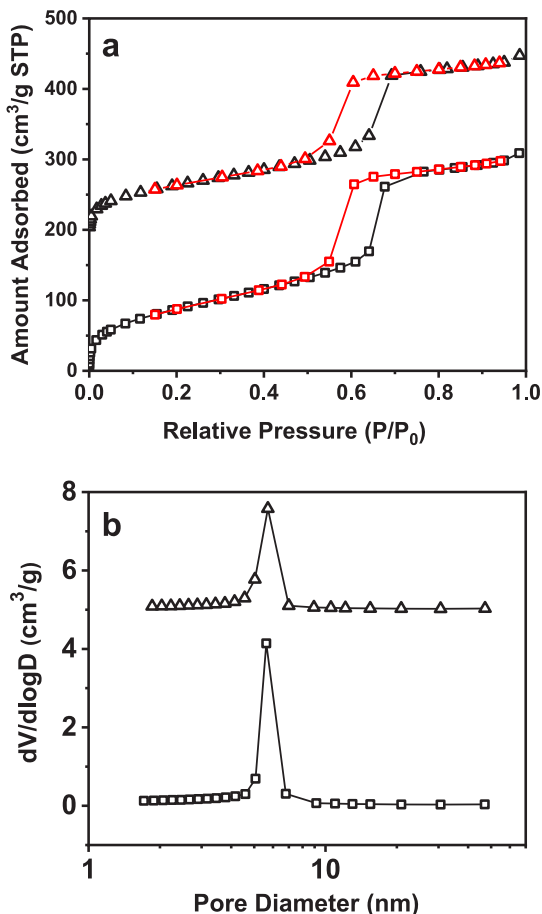


Figure 3. N<sub>2</sub> adsorption and desorption isotherms and BJH pore size distribution of NH2-SBA-15-cal (□) and NH2-SBA-15-IL (△) at  $-196\text{ }^{\circ}\text{C}$ . Isotherms for NH2-SBA-15-IL and BJH pore size distributions were offset by 200 cm<sup>3</sup>/g STP and 5 cm<sup>3</sup>/g for clarity.

desorption isotherms at  $-196\text{ }^{\circ}\text{C}$  of NH2-SBA-15-cal and NH2-SBA-15-IL. The BET surface area and total pore volume of the amine grafted samples are much lower than those of pristine SBA-15. This decrease can be attributed to the partial pore blockage and increased weight from the grafted 3-aminopropyl groups. The BJH pore size distributions were centered at 5.6 and 5.7 nm for NH2-SBA-15-cal and NH2-SBA-15-IL, respectively. The change of pore size of SBA-15-IL after amine grafting (from 7.5 to 5.7 nm) is larger than that of SBA-15-cal (from 6.4 to 5.6 nm), which suggests the possibility of higher amine loading for NH2-SBA-15-IL.

To investigate the amine loadings on NH2-SBA-15-cal and NH2-SBA-15-IL, the samples were analyzed by TGA in air flow. Both samples were degassed in helium *in situ* to remove

adsorbed moisture and CO<sub>2</sub> before analysis. As shown in Figure 4, NH2-SBA-15-IL showed a total 24.2% weight loss

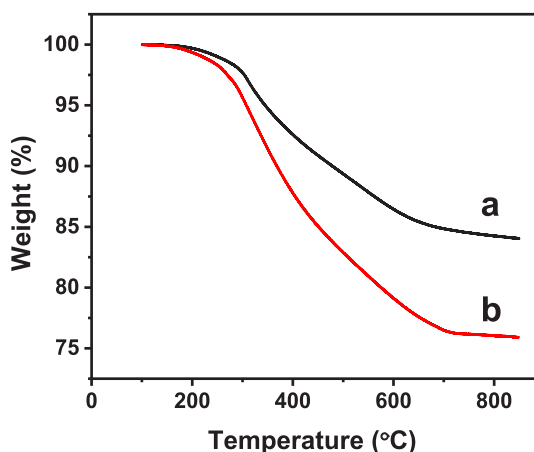


Figure 4. TGA thermograms of (a) NH2-SBA-15-cal and (b) NH2-SBA-15-IL in an air flow.

under air atmosphere. For NH2-SBA-15-cal, the total weight loss was 16.0%. The weight loss difference between NH2-SBA-15-cal and NH2-SBA-15-IL indicated 51% more amine was grafted on SBA-15-IL. According to previous studies,<sup>19</sup> the bidentate grafting is more likely to happen than the tridentate grafting. Based on the weight loss result and considering the complete removal of the 3-aminopropyl group and a methoxyl group, the amine loadings were estimated to be 1.4 mmol/g for NH2-SBA-15-cal and 2.2 mmol/g for NH2-SBA-15-IL. These results confirmed that more amine groups were grafted on SBA-15-IL than on conventional thermal template removal sample SBA-15-cal, which is in accordance with pore size distribution of NH2-SBA-15-IL.

**CO<sub>2</sub> Capture Performance.** The CO<sub>2</sub> and N<sub>2</sub> adsorption isotherms on NH2-SBA-15-cal and NH2-SBA-15-IL are compared in Figure 5. At 760 Torr (1 atm), the amount of CO<sub>2</sub> adsorbed was 1.8 mmol/g for NH2-SBA-15-IL and 1.3 mmol/g for NH2-SBA-15-cal, while for N<sub>2</sub> adsorbed it was 0.04 mmol/g on NH2-SBA-15-IL and 0.08 mmol/g on NH2-SBA-15-cal. For CO<sub>2</sub> adsorption on both amine grafted samples, the isotherms showed steep increases in the low

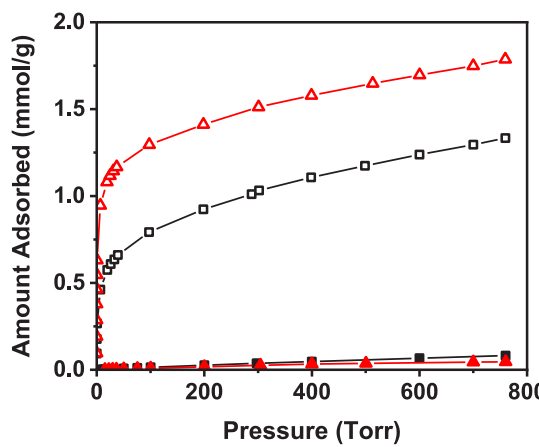


Figure 5. CO<sub>2</sub> adsorption isotherms on amine grafted SBA-15-cal (□) and amine grafted SBA-15-IL (△) at 25 °C. The closed symbol is the N<sub>2</sub> adsorption isotherms at 25 °C.

pressure range. The steep increase in the low pressure range on the amine grafted samples correlates with the strong interactions between the primary amine groups ( $-\text{NH}_2$ ) grafted on SBA-15 and the  $\text{CO}_2$  molecules.<sup>22,46</sup> Based on the grafted amine loadings determined by TGA, the amine efficiencies of  $\text{CO}_2/\text{N}$  near the “knees” of the  $\text{CO}_2$  isotherms are about 0.5, in agreement with the ratio of  $\text{CO}_2$  and amine groups to form a carbamate. The high amount of  $\text{CO}_2$  adsorbed at low pressure on NH2-SBA-15-IL makes it a good adsorbent for  $\text{CO}_2$  capture from dilute gases or direct air capture; the results will be discussed subsequently.

Adsorption of  $\text{CO}_2$  from flue gas or postcombustion gas is perhaps the most common application of carbon capture and storage (CCS) currently. Considering the conditions relevant to flue gas ( $\sim 15\% \text{CO}_2$  concentration and 80%  $\text{N}_2$  concentration), the  $\text{CO}_2$  capacity of NH2-SBA-15-IL (1.3 mmol/g at 114 Torr, 0.15 atm) was 63% more than that of NH2-SBA-15-cal (0.8 mmol/g at 114 Torr, 0.15 atm). The corresponding pure-component selectivity of  $\text{CO}_2$  over  $\text{N}_2$  for NH2-SBA-15-IL was 36 (calculated by using  $\text{CO}_2$  capacity at 0.15 atm and  $\text{N}_2$  capacity at 0.8 atm), about 3 times the  $\text{CO}_2$  over  $\text{N}_2$  pure-component selectivity for NH2-SBA-15-cal. Compared with other template extraction methods, such as ethanol extraction, the  $\text{CO}_2$  capacity increase of NH2-SBA-15-IL under flue gas conditions is higher than that of ethanol extraction sample (an increase of 52%  $\text{CO}_2$  adsorption capacity compared with the conventional calcined sample).<sup>22</sup> The results indicate that the novel ionic liquid template removal method is a better template extraction method to increase the  $\text{CO}_2$  adsorption capacity and the  $\text{CO}_2/\text{N}_2$  selectivity.

The  $\text{CO}_2$  adsorption isotherms on NH2-SBA-15-cal and NH2-SBA-15-IL were also investigated at 40 and 70 °C (Figure 6). The  $\text{CO}_2$  capacity decreased with temperature on both amine grafted samples. The isosteric heats of adsorption on NH2-SBA-15-cal and NH2-SBA-15-IL were calculated from the  $\text{CO}_2$  isotherms at 25, 40, and 70 °C by using the Clausius–Clapeyron equation and are compared in Figure 7. The isosteric heats of adsorption were determined by evaluating the slope of the plot of  $\ln(P)$  versus  $1/T$  at the same  $\text{CO}_2$  adsorbed amount. As shown in Figure 7, the heats of adsorption on NH2-SBA-15-cal decreased from 77 kJ/mol (at 0.1 mmol/g  $\text{CO}_2$  adsorbed amount) to 28 kJ/mol (at 0.9 mmol/g). For NH2-SBA-15-IL, the heats of adsorption declined from 90 kJ/mol (at 0.25 mmol/g  $\text{CO}_2$  adsorbed amount) to 62 kJ/mol (at 1.0 mmol/g). At the same amount of  $\text{CO}_2$  adsorbed, the heat of adsorption value of NH2-SBA-15-IL is higher than that of NH2-SBA-15-cal. The previous TGA results showed that the amine loading on NH2-SBA-15-IL is higher than that on NH2-SBA-15-cal. These results agreed with previous studies, which showed the heats of adsorption of amine grafted samples increased as the amine loading was increased.<sup>17,22</sup> It is noted that the heat of adsorption value for NH2-SBA-15-cal at the  $\text{CO}_2$  adsorbed amount of 0.7 mmol/g was already below 40 kJ/mol, indicating the physisorption of  $\text{CO}_2$  on silicas was beginning to occur. At the same  $\text{CO}_2$  adsorbed amount (0.7 mmol/g), the heat of adsorption value for NH2-SBA-15-IL was 81 kJ/mol, meaning the  $\text{CO}_2$  adsorbed on NH2-SBA-15-IL was still reacting with amine groups. The high isosteric heat of adsorption on NH2-SBA-15-IL led to the enhanced  $\text{CO}_2$  adsorption capacity.

From the  $\text{CO}_2$  isotherms at low concentration (Figure 8), NH2-SBA-15-IL demonstrated a  $\text{CO}_2$  capacity more than twice that of amine grafted conventional template removal

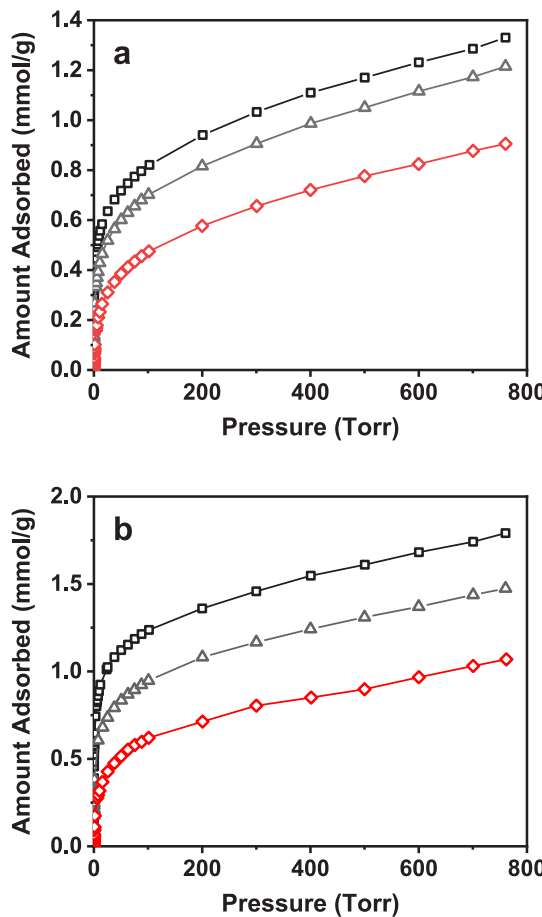


Figure 6.  $\text{CO}_2$  adsorption isotherms on NH2-SBA-15-cal (a) and NH2-SBA-15-IL (b) at 25 (□), 40 (△), and 70 °C (◇).

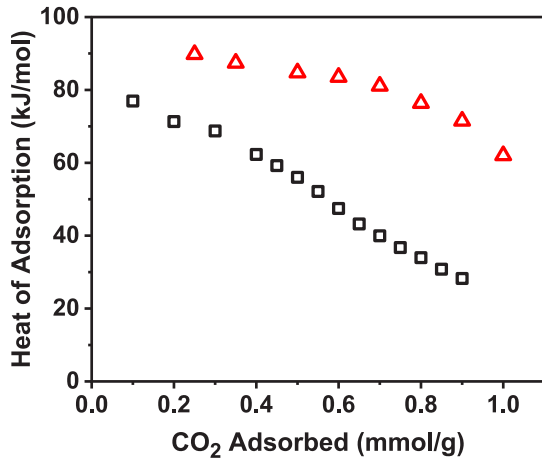


Figure 7. Isosteric heats of adsorption versus  $\text{CO}_2$  loading for NH2-SBA-15-cal (□) and NH2-SBA-15-IL (△).

sample NH2-SBA-15-cal. The much higher  $\text{CO}_2$  adsorption capacities of NH2-SBA-15-IL at low  $\text{CO}_2$  concentrations indicate this adsorbent would be well-suited for  $\text{CO}_2$  capture from an ultradilute gas stream such as ambient air.

Fixed-bed breakthrough experiments were performed on NH2-SBA-15-cal and NH2-SBA-15-IL using both dry and wet ambient air feeds (relative humidity of 60% when wet) to study the working capacities under air capture conditions. Feed gas hourly space velocities (GHSV) of 4200 h<sup>-1</sup> were used for the

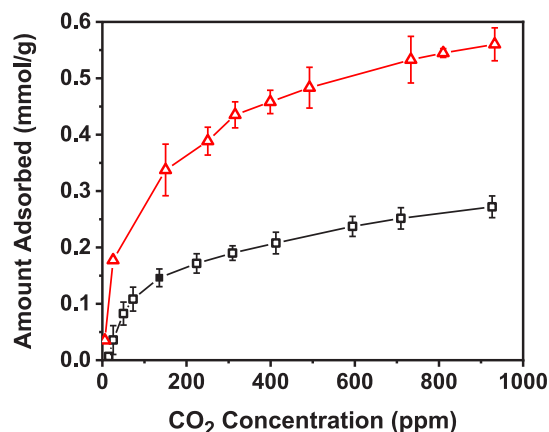


Figure 8. Low concentration CO<sub>2</sub> adsorption isotherms on amine grafted SBA-15-cal (□) and amine grafted SBA-15-IL (Δ) at 25 °C.

adsorbent beds. As shown in Figure 9, both NH<sub>2</sub>-SBA-15-cal and NH<sub>2</sub>-SBA-15-IL showed sharp breakthrough curves,

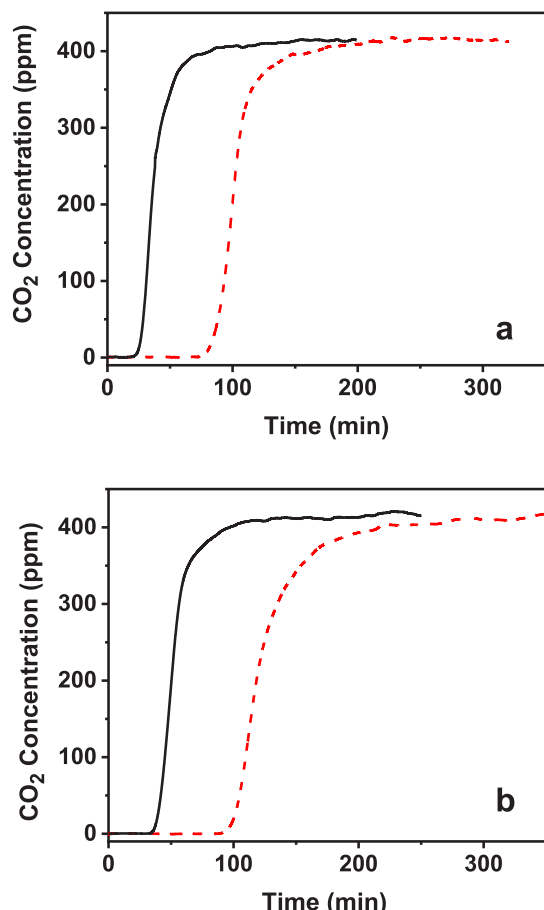


Figure 9. CO<sub>2</sub> breakthrough curves of NH<sub>2</sub>-SBA-15-cal (solid lines) and NH<sub>2</sub>-SBA-15-IL (dashed lines) for ambient air with 415 ppm CO<sub>2</sub> at 1 atm and 25 °C: (a) dry conditions; (b) wet conditions, RH 60%.

which indicated the fast mass transfer in the adsorbent beds. The calculated fixed-bed breakthrough capacities of NH<sub>2</sub>-SBA-15-cal for direct air capture (ambient air with 415 ppm CO<sub>2</sub> at 25 °C) were 0.146 mmol/g under dry conditions and 0.196 mmol/g under wet conditions. For NH<sub>2</sub>-SBA-15-IL, the

breakthrough capacities under dry and wet conditions were 0.375 and 0.456 mmol/g, respectively. The increased CO<sub>2</sub> capacities under wet conditions are typical for amine-functionalized silicas. Under dry conditions, two amine groups are needed to react with one CO<sub>2</sub> molecule to form a carbamate. One amine group can react with one CO<sub>2</sub> molecule to form a bicarbonate in the presence of water (wet conditions).<sup>21,47</sup> It is noted that NH<sub>2</sub>-SBA-15-IL showed a higher increase in CO<sub>2</sub> capacity when comparing dry and wet conditions than NH<sub>2</sub>-SBA-15-cal. Such findings are consistent with the previously reported study that lower surface amine coverage silicas showed more pronounced enhancement for amine efficiency in humid adsorption conditions.<sup>48</sup> The working (breakthrough) capacities of both adsorbents are lower than the equilibrium capacities measured by the volumetric method. The lower working capacities might be due to the competing adsorption with nitrogen and other gases and also the high GHSV that was used in the breakthrough experiments.<sup>43</sup> The significantly higher fixed-bed breakthrough capacity of NH<sub>2</sub>-SBA-15-IL makes this adsorbent promising for capturing CO<sub>2</sub> directly from ambient air, i.e., for direct air capture.

For practical applications, the stability of the adsorbents is a critical factor for CO<sub>2</sub> capture since it affects the cost of the overall process. The multicycle stability of NH<sub>2</sub>-SBA-15-IL was investigated by cyclic temperature swing adsorption/desorption cycles. As shown in Figure 10, all cycles took less

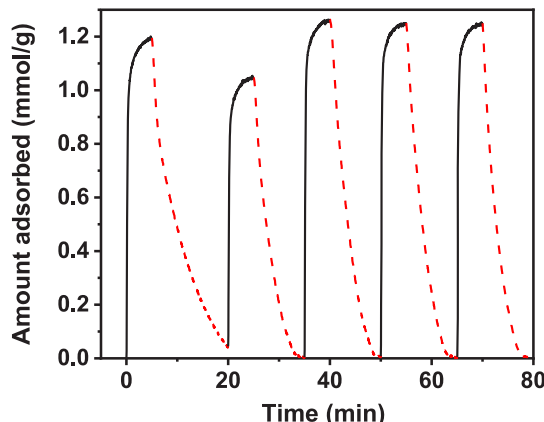
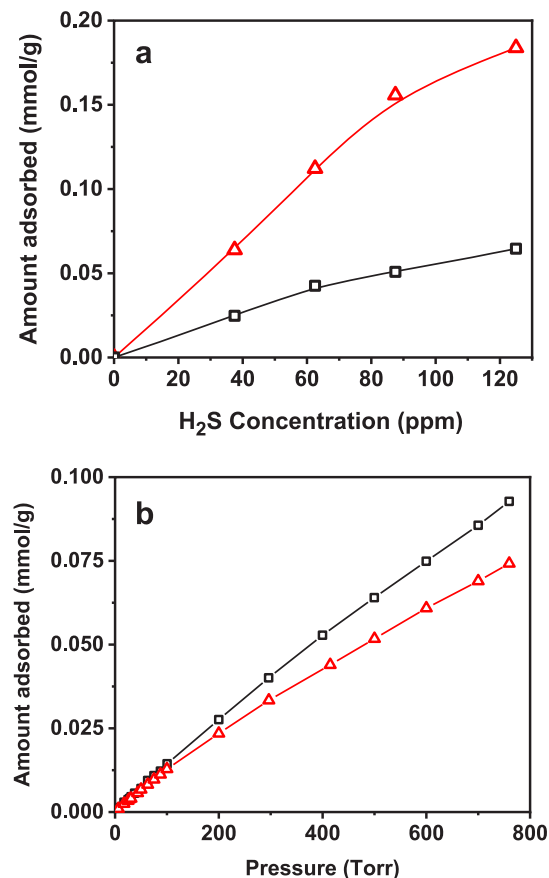


Figure 10. Multicycle TGA adsorption curves of NH<sub>2</sub>-SBA-15-IL at 25 °C in CO<sub>2</sub> flow (70% in helium, solid lines) and desorption curves in helium at 90 °C (dashed lines).

than 5 min to reach the “knee” of the adsorption curves, and CO<sub>2</sub> desorbed completely in less than 10 min (the first cycle took 15 min). After the first two cycles, there were no significant changes in CO<sub>2</sub> adsorption capacities for NH<sub>2</sub>-SBA-15-IL at 25 °C, which indicates that NH<sub>2</sub>-SBA-15-IL exhibited good multicycle stability. The lower capacities of the first two cycles can be attributed to lower temperature and shorter time used for pretreating the adsorbent before the multicycle experiments. The surface of the adsorbent became more thoroughly regenerated after the first two cycles, and the adsorbent showed cyclic steady state in the ensuing three cycles.

**H<sub>2</sub>S Capture Performance.** H<sub>2</sub>S is a toxic, acidic gas that needs to be removed from natural gas. The allowable limit for “pipeline grade” methane in the United States is 4 ppm.<sup>49</sup> Therefore, desulfurization is an important step in the natural

gas processing industry. The adsorption isotherms of low concentration  $\text{H}_2\text{S}$  and pure methane on NH2-SBA-15-cal and NH2-SBA-15-IL are shown in Figure 11. The adsorption rates



**Figure 11.** Adsorption isotherms of  $\text{H}_2\text{S}$  (a) and  $\text{CH}_4$  (b) adsorption isotherms on amine grafted SBA-15-cal (□) and amine grafted SBA-15-IL (△) at 25 °C.

of  $\text{H}_2\text{S}$  on amine grafted samples were considerably slower than that of  $\text{CO}_2$ . The concentration of  $\text{H}_2\text{S}$  was increased every 120 min to acquire each data point to approximate the  $\text{H}_2\text{S}$  “equilibrium” isotherm. At 125 ppm, the amounts of  $\text{H}_2\text{S}$  adsorbed were 0.06 and 0.18 mmol/g for NH2-SBA-15-cal and NH2-SBA-15-IL, respectively. The amounts of methane adsorbed (at 760 Torr) on NH2-SBA-15-cal and NH2-SBA-15-IL were 0.09 and 0.07 mmol/g, respectively. The pure-component selectivity of  $\text{H}_2\text{S}$  over methane for NH2-SBA-15-IL was 2.6 (calculated by using  $\text{H}_2\text{S}$  capacity at 125 ppm and methane capacity at 1 atm), making the adsorbent applicable for desulfurization by pressure swing adsorption (PSA).<sup>50</sup> The high adsorption capacity at low  $\text{H}_2\text{S}$  concentration and the largely improved  $\text{H}_2\text{S}$ /methane selectivity indicate that NH2-SBA-15-IL is a promising adsorbent for removal of traces of  $\text{H}_2\text{S}$  in natural gas.

All selectivities mentioned in this work refer to single-component selectivities. All known models for predicting mixed-gas adsorption selectivities from single-gas isotherms have been discussed by Yang.<sup>50</sup> Ritter and Yang studied pure and mixed-gas adsorption on carbon for gases containing  $\text{CO}_2$  and  $\text{H}_2\text{S}$  (i.e.,  $\text{H}_2\text{S}/\text{CO}_2/\text{CH}_4/\text{H}_2/\text{CO}$ ) and concluded that all models deviated substantially (by >50%) from experimental mixed-gas data. It is particularly relevant that the two gases that

adsorb most strongly, i.e.,  $\text{H}_2\text{S}$  and  $\text{CO}_2$ , dominated the adsorbed phase causing the highest deviation.<sup>51</sup>

**Mechanism for Template Removal by Ionic Liquid, and Recovery/Reuse of I.L. and P123.** To understand the mechanism for template removal by ionic liquid treatment, P123 and 1-*n*-butyl-3-methylimidazolium chloride (I.L.) were recovered using carbon tetrachloride ( $\text{CCl}_4$ ) and deuterated chloroform ( $\text{CDCl}_3$ ) at room temperature, respectively.  $\text{CCl}_4$  selectively dissolves organic template P123. After the dissolution of P123 from the acquired mixtures after ionic liquid treatment,  $\text{CDCl}_3$  was used to extract 1-*n*-butyl-3-methylimidazolium chloride. Deuterated solvent was used to avoid the mix with solvent signals and compound signals, which might lead to misinterpretation. The  $^1\text{H}$  NMR spectra of I.L. before and after template removal process were compared in Figure 12, and it also shows the comparison for the organic template P123. The structures of I.L. and P123 did not change upon the template removal (no new peaks or disappeared peaks after template removal), suggesting that P123 did not decompose during the ionic liquid treatment. For as-synthesized SBA-15, the interactions between the surface of the silica walls and the P123 template are H-bonding interactions between silanols and the EO moiety of P123.<sup>52,53</sup> The mechanism of cellulose dissolution in the ionic liquid 1-*n*-butyl-3-methylimidazolium chloride is the disruption of the hydrogen bonding network in cellulose.<sup>34</sup> Based on the results stated above, the mechanism of template removal via ionic liquid treatment was likely due to breakage of hydrogen bonds between the template P123 and the silanol groups on the surface of as-synthesized SBA-15. As a result, the silanol groups on the surface of SBA-15 were greatly preserved during the template removal process, which explains the high surface hydroxyl group density of SBA-15-IL. Moreover, due to the unchanged structures of template P123 and I.L. during ionic liquid treatment, both P123 and ionic liquid can be recovered and reused, which makes the ionic liquid treatment method commercially viable for template removal of SBA-15. The solvent to be used for extraction of I.L. ( $\text{CDCl}_3$ ) would be replaced by chloroform ( $\text{CHCl}_3$ ) or acetone to reduce the cost for commercial processing.

As mentioned, the mechanism of template removal via ionic liquid treatment might be similar to the mechanism of cellulose dissolution in ionic liquids. Therefore, ionic liquids with better cellulose solubilities and lower melting points might preserve more silanol groups during the treatment. Investigation on the possibility of template removal via ionic liquid treatment under room temperature is in progress.

## CONCLUSIONS

Extraction with ionic liquid has been successfully applied for efficient template removal from mesoporous SBA-15. Ionic liquid treatment removes the template by breaking the hydrogen bonds between the silanol groups on the SBA-15 surface and the organic template P123. Compared with conventional air calcination, ionic liquid treatment helped to preserve silanol groups on the SBA-15 surface and prevent structure shrinkage, resulting in a larger amount of grafted amine which consequently led to higher  $\text{CO}_2$  and  $\text{H}_2\text{S}$  adsorption capacities and selectivities. Fixed-bed  $\text{CO}_2$  breakthrough experiments with ambient air performed under dry and wet conditions indicate that amine grafted SBA-15 by the ionic liquid treatment template removal method (NH2-SBA-15-IL) is also a promising adsorbent for direct air capture. The

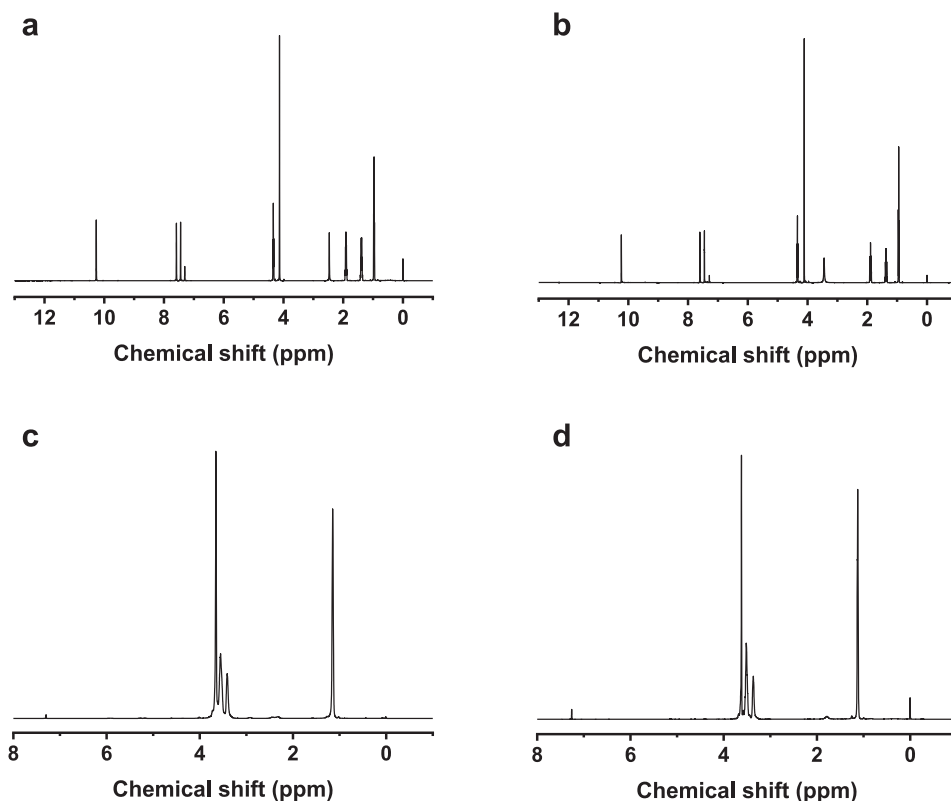


**Figure 12.**  $^1\text{H}$  NMR spectrum of (a) 1-*n*-butyl-3-methylimidazolium chloride (I.L.); (b) recovered I.L. after template removal; (c) P123 (template); (d) recovered P123 template after template removal.

stability of NH<sub>2</sub>-SBA-15-IL is confirmed by a multicycle CO<sub>2</sub> adsorption/desorption test.

## ■ ASSOCIATED CONTENT

### ● Supporting Information

The Supporting Information is available free of charge at <https://pubs.acs.org/doi/10.1021/acssuschemeng.0c01941>.

Possibilities of lowering the temperature of ionic liquid treatment; CO<sub>2</sub> isotherms of samples treated under different temperatures (PDF)

## ■ AUTHOR INFORMATION

### Corresponding Author

Ralph T. Yang – Department of Chemical Engineering,  
University of Michigan, Ann Arbor, Michigan 48109, United  
States;  [orcid.org/0000-0002-5367-9550](https://orcid.org/0000-0002-5367-9550); Email: [yang@umich.edu](mailto:yang@umich.edu)

### Author

Yiren Wang – Department of Chemical Engineering, University  
of Michigan, Ann Arbor, Michigan 48109, United States

Complete contact information is available at:

<https://pubs.acs.org/10.1021/acssuschemeng.0c01941>

### Notes

The authors declare no competing financial interest.

## ■ ACKNOWLEDGMENTS

Funding from China Scholarship Council, University of Michigan BlueSky Global CO<sub>2</sub> Initiative, and NSF CBET-1826621 is gratefully acknowledged.

## ■ REFERENCES

- (1) Bezerra, D. P.; Oliveira, R. S.; Vieira, R. S.; Cavalcante, C. L.; Azevedo, D. C. S. Adsorption of CO<sub>2</sub> on nitrogen-enriched activated carbon and zeolite 13X. *Adsorption* **2011**, *17* (1), 235–246.
- (2) Wang, L.; Yang, R. T. Significantly Increased CO<sub>2</sub> Adsorption Performance of Nanostructured Templated Carbon by Tuning Surface Area and Nitrogen Doping. *J. Phys. Chem. C* **2012**, *116* (1), 1099–1106.
- (3) Wu, Z.; Webley, P. A.; Zhao, D. Post-enrichment of nitrogen in soft-templated ordered mesoporous carbon materials for highly efficient phenol removal and CO<sub>2</sub> capture. *J. Mater. Chem.* **2012**, *22* (22), 11379–11389.
- (4) Moran, C. M.; Marti, R. M.; Joshi, J. N.; Hayes, S. E.; Walton, K. S. Tuning residual metal in partially etched carbide-derived carbons for enhanced acid gas adsorption. *Carbon* **2020**, *158*, 481–493.
- (5) Kennedy, D. A.; Tezel, F. H. Cation exchange modification of clinoptilolite - Screening analysis for potential equilibrium and kinetic adsorption separations involving methane, nitrogen, and carbon dioxide. *Microporous Mesoporous Mater.* **2018**, *262*, 235–250.
- (6) Moura, P. A. S.; Bezerra, D. P.; Vilarrasa-Garcia, E.; Bastos-Neto, M.; Azevedo, D. C. S. Adsorption equilibria of CO<sub>2</sub> and CH<sub>4</sub> in cation-exchanged zeolites 13X. *Adsorption* **2016**, *22* (1), 71–80.
- (7) Shang, J.; Li, G.; Singh, R.; Gu, Q.; Nairn, K. M.; Bastow, T. J.; Medhekar, N.; Doherty, C. M.; Hill, A. J.; Liu, J. Z.; Webley, P. A. Discriminative Separation of Gases by a “Molecular Trapdoor” Mechanism in Chabazite Zeolites. *J. Am. Chem. Soc.* **2012**, *134* (46), 19246–19253.
- (8) Kennedy, D. A.; Mujčin, M.; Abou-Zeid, C.; Tezel, F. H. Cation exchange modification of clinoptilolite -thermodynamic effects on adsorption separations of carbon dioxide, methane, and nitrogen. *Microporous Mesoporous Mater.* **2019**, *274*, 327–341.
- (9) Zhao, Q.; Wu, F.; Men, Y.; Fang, X.; Zhao, J.; Xiao, P.; Webley, P. A.; Grande, C. A. CO<sub>2</sub> capture using a novel hybrid monolith (H-

ZSMS/activated carbon) as adsorbent by combined vacuum and electric swing adsorption (VESA). *Chem. Eng. J.* **2019**, *358*, 707–717.

(10) Jasuja, H.; Walton, K. S. Experimental Study of CO<sub>2</sub>, CH<sub>4</sub>, and Water Vapor Adsorption on a Dimethyl-Functionalized UiO-66 Framework. *J. Phys. Chem. C* **2013**, *117* (14), 7062–7068.

(11) Karra, J. R.; Grabicka, B. E.; Huang, Y.; Walton, K. S. Adsorption study of CO<sub>2</sub>, CH<sub>4</sub>, N<sub>2</sub>, and H<sub>2</sub>O on an interwoven copper carboxylate metal-organic framework (MOF-14). *J. Colloid Interface Sci.* **2013**, *392*, 331–336.

(12) Cavenati, S.; Grande, C. A.; Rodrigues, A. E.; Kiener, C.; Müller, U. Metal Organic Framework Adsorbent for Biogas Upgrading. *Ind. Eng. Chem. Res.* **2008**, *47* (16), 6333–6335.

(13) Liu, F.; Huang, K.; Yoo, C.; Okonkwo, C.; Tao, D.; Jones, C. W.; Dai, S. Facilely synthesized meso-macroporous polymer as support of poly(ethyleneimine) for highly efficient and selective capture of CO<sub>2</sub>. *Chem. Eng. J.* **2017**, *314*, 466–476.

(14) Huang, K.; Liu, F.; Dai, S. Solvothermal synthesis of hierarchically nanoporous organic polymers with tunable nitrogen functionality for highly selective capture of CO<sub>2</sub>. *J. Mater. Chem. A* **2016**, *4* (34), 13063–13070.

(15) Liu, F.; Huang, K.; Wu, Q.; Dai, S. Solvent-Free Self-Assembly to the Synthesis of Nitrogen-Doped Ordered Mesoporous Polymers for Highly Selective Capture and Conversion of CO<sub>2</sub>. *Adv. Mater.* **2017**, *29* (27), 1700445.

(16) Mi, J.; Liu, F.; Chen, W.; Chen, X.; Shen, L.; Cao, Y.; Au, C.; Huang, K.; Zheng, A.; Jiang, L. Design of Efficient, Hierarchical Porous Polymers Endowed with Tunable Structural Base Sites for Direct Catalytic Elimination of COS and H<sub>2</sub>S. *ACS Appl. Mater. Interfaces* **2019**, *11* (33), 29950–29959.

(17) Alkhabbaz, M. A.; Bollini, P.; Foo, G. S.; Sievers, C.; Jones, C. W. Important Roles of Enthalpic and Entropic Contributions to CO<sub>2</sub> Capture from Simulated Flue Gas and Ambient Air Using Mesoporous Silica Grafted Amines. *J. Am. Chem. Soc.* **2014**, *136* (38), 13170–13173.

(18) Bollini, P.; Brunelli, N. A.; Didas, S. A.; Jones, C. W. Dynamics of CO<sub>2</sub> Adsorption on Amine Adsorbents. 1. Impact of Heat Effects. *Ind. Eng. Chem. Res.* **2012**, *51* (46), 15145–15152.

(19) Bollini, P.; Brunelli, N. A.; Didas, S. A.; Jones, C. W. Dynamics of CO<sub>2</sub> Adsorption on Amine Adsorbents. 2. Insights Into Adsorbent Design. *Ind. Eng. Chem. Res.* **2012**, *51* (46), 15153–15162.

(20) Darunte, L. A.; Sen, T.; Bhawanani, C.; Walton, K. S.; Sholl, D. S.; Realff, M. J.; Jones, C. W. Moving Beyond Adsorption Capacity in Design of Adsorbents for CO<sub>2</sub> Capture from Ultradilute Feeds: Kinetics of CO<sub>2</sub> Adsorption in Materials with Stepped Isotherms. *Ind. Eng. Chem. Res.* **2019**, *58* (1), 366–377.

(21) Huang, H. Y.; Yang, R. T.; Chinn, D.; Munson, C. L. Amine-Grafted MCM-48 and Silica Xerogel as Superior Sorbents for Acidic Gas Removal from Natural Gas. *Ind. Eng. Chem. Res.* **2003**, *42* (12), 2427–2433.

(22) Wang, L.; Yang, R. T. Increasing Selective CO<sub>2</sub> Adsorption on Amine-Grafted SBA-15 by Increasing Silanol Density. *J. Phys. Chem. C* **2011**, *115* (43), 21264–21272.

(23) Yuan, M.; Wang, L.; Yang, R. T. Glow Discharge Plasma-Assisted Template Removal of SBA-15 at Ambient Temperature for High Surface Area, High Silanol Density, and Enhanced CO<sub>2</sub> Adsorption Capacity. *Langmuir* **2014**, *30* (27), 8124–8130.

(24) Kan, X.; Chen, X.; Chen, W.; Mi, J.; Zhang, J.; Liu, F.; Zheng, A.; Huang, K.; Shen, L.; Au, C.; Jiang, L. Nitrogen-Decorated, Ordered Mesoporous Carbon Spheres as High-Efficient Catalysts for Selective Capture and Oxidation of H<sub>2</sub>S. *ACS Sustainable Chem. Eng.* **2019**, *7* (8), 7609–7618.

(25) Mi, J.; Chen, X.; Zhang, Q.; Zheng, Y.; Xiao, Y.; Liu, F.; Au, C.; Jiang, L. Mechanochemically synthesized MgAl layered double hydroxide nanosheets for efficient catalytic removal of carbonyl sulfide and H<sub>2</sub>S. *Chem. Commun.* **2019**, *55* (63), 9375–9378.

(26) Wang, L.; Yang, R. T. New nanostructured sorbents for desulfurization of natural gas. *Front. Chem. Sci. Eng.* **2014**, *8* (1), 8–19.

(27) Kresge, C. T.; Leonowicz, M. E.; Roth, W. J.; Vartuli, J. C.; Beck, J. S. Ordered mesoporous molecular sieves synthesized by a liquid-crystal template mechanism. *Nature* **1992**, *359* (6397), 710–712.

(28) Zhao, D.; Feng, J.; Huo, Q.; Melosh, N.; Fredrickson, G. H.; Chmelka, B. F.; Stucky, G. D. Triblock Copolymer Syntheses of Mesoporous Silica with Periodic 50 to 300 Angstrom Pores. *Science* **1998**, *279* (5350), 548–552.

(29) Zhao, D.; Huo, Q.; Feng, J.; Chmelka, B. F.; Stucky, G. D. Nonionic Triblock and Star Diblock Copolymer and Oligomeric Surfactant Syntheses of Highly Ordered, Hydrothermally Stable, Mesoporous Silica Structures. *J. Am. Chem. Soc.* **1998**, *120* (24), 6024–6036.

(30) Taney, P. T.; Pinnavaia, T. J. A Neutral Templating Route to Mesoporous Molecular Sieves. *Science* **1995**, *267* (5199), 865–867.

(31) Xiao, L.; Li, J.; Jin, H.; Xu, R. Removal of organic templates from mesoporous SBA-15 at room temperature using UV/dilute H<sub>2</sub>O<sub>2</sub>. *Microporous Mesoporous Mater.* **2006**, *96* (1), 413–418.

(32) van Grieken, R.; Calleja, G.; Stucky, G. D.; Melero, J. A.; García, R. A.; Iglesias, J. Supercritical Fluid Extraction of a Nonionic Surfactant Template from SBA-15 Materials and Consequences on the Porous Structure. *Langmuir* **2003**, *19* (9), 3966–3973.

(33) Tian, B.; Liu, X.; Yu, C.; Gao, F.; Luo, Q.; Xie, S.; Tu, B.; Zhao, D. Microwave assisted template removal of siliceous porous materials. *Chem. Commun.* **2002**, No. 11, 1186–1187.

(34) Remsing, R. C.; Swatloski, R. P.; Rogers, R. D.; Moyna, G. Mechanism of cellulose dissolution in the ionic liquid 1-n-butyl-3-methylimidazolium chloride: a <sup>13</sup>C and 35/37Cl NMR relaxation study on model systems. *Chem. Commun.* **2006**, No. 12, 1271–1273.

(35) Swatloski, R. P.; Spear, S. K.; Holbrey, J. D.; Rogers, R. D. Dissolution of Cellose with Ionic Liquids. *J. Am. Chem. Soc.* **2002**, *124* (18), 4974–4975.

(36) Usmani, Z.; Sharma, M.; Gupta, P.; Karpichev, Y.; Gathergood, N.; Bhat, R.; Gupta, V. K. Ionic liquid based pretreatment of lignocellulosic biomass for enhanced bioconversion. *Bioresour. Technol.* **2020**, *304*, 123003.

(37) Brennecke, J. F.; Gurkan, B. E. Ionic Liquids for CO<sub>2</sub> Capture and Emission Reduction. *J. Phys. Chem. Lett.* **2010**, *1* (24), 3459–3464.

(38) Myers, C.; Pennline, H.; Luebke, D.; Ilconich, J.; Dixon, J. K.; Maginn, E. J.; Brennecke, J. F. High temperature separation of carbon dioxide/hydrogen mixtures using facilitated supported ionic liquid membranes. *J. Membr. Sci.* **2008**, *322* (1), 28–31.

(39) Liu, F.; Chen, W.; Mi, J.; Zhang, J.; Kan, X.; Zhong, F.; Huang, K.; Zheng, A.; Jiang, L. Thermodynamic and molecular insights into the absorption of H<sub>2</sub>S, CO<sub>2</sub>, and CH<sub>4</sub> in choline chloride plus urea mixtures. *AIChE J.* **2019**, *65* (5), No. e16574.

(40) Liu, F.; Huang, K.; Jiang, L. Promoted adsorption of CO<sub>2</sub> on amine-impregnated adsorbents by functionalized ionic liquids. *AIChE J.* **2018**, *64* (10), 3671–3680.

(41) Plechkova, N. V.; Seddon, K. R. Applications of ionic liquids in the chemical industry. *Chem. Soc. Rev.* **2008**, *37* (1), 123–150.

(42) Weingärtner, H. Understanding Ionic Liquids at the Molecular Level: Facts, Problems, and Controversies. *Angew. Chem., Int. Ed.* **2008**, *47* (4), 654–670.

(43) Stuckert, N. R.; Yang, R. T. CO<sub>2</sub> Capture from the Atmosphere and Simultaneous Concentration Using Zeolites and Amine-Grafted SBA-15. *Environ. Sci. Technol.* **2011**, *45* (23), 10257–10264.

(44) Anyanwu, J.-T.; Wang, Y.; Yang, R. T. Amine-Grafted Silica Gels for CO<sub>2</sub> Capture Including Direct Air Capture. *Ind. Eng. Chem. Res.* **2020**, *59* (15), 7072–7079.

(45) Thommes, M.; Kaneko, K.; Neimark, A. V.; Olivier, J. P.; Rodriguez-Reinoso, F.; Rouquerol, J.; Sing, K. S. W. Physisorption of gases, with special reference to the evaluation of surface area and pore size distribution (IUPAC Technical Report). *Pure Appl. Chem.* **2015**, *87* (9–10), 1051–1069.

(46) Danon, A.; Stair, P. C.; Weitz, E. FTIR Study of CO<sub>2</sub> Adsorption on Amine-Grafted SBA-15: Elucidation of Adsorbed Species. *J. Phys. Chem. C* **2011**, *115* (23), 11540–11549.

(47) Chen, C.; Shimon, D.; Lee, J. J.; Mentink-Vigier, F.; Hung, I.; Sievers, C.; Jones, C. W.; Hayes, S. E. The “Missing” Bicarbonate in CO<sub>2</sub> Chemisorption Reactions on Solid Amine Sorbents. *J. Am. Chem. Soc.* **2018**, *140* (28), 8648–8651.

(48) Didas, S. A.; Sakwa-Novak, M. A.; Foo, G. S.; Sievers, C.; Jones, C. W. Effect of Amine Surface Coverage on the Co-Adsorption of CO<sub>2</sub> and Water: Spectral Deconvolution of Adsorbed Species. *J. Phys. Chem. Lett.* **2014**, *5* (23), 4194–4200.

(49) Häring, H.-W. *Industrial Gas Processing*; Wiley-VCH: Weinheim, Germany, 2008.

(50) Yang, R. T. *Gas Separation by Adsorption Processes*; Imperial College Press: London, U.K., 1997.

(51) Ritter, J. A.; Yang, R. T. Equilibrium adsorption of multicomponent gas mixtures at elevated pressures. *Ind. Eng. Chem. Res.* **1987**, *26* (8), 1679–1686.

(52) Pan, D.; Zhao, L.; Qian, K.; Tan, L.; Zhou, L.; Zhang, J.; Huang, X.; Fan, Y.; Liu, H.; Yu, C.; Bao, X. A silanol protection mechanism: Understanding the decomposition behavior of surfactants in mesostructured solids. *J. Mater. Res.* **2011**, *26* (6), 804–814.

(53) Xiao, N.; Wang, L.; Liu, S.; Zou, Y.; Wang, C.; Ji, Y.; Song, J.; Li, F.; Meng, X.; Xiao, F. High-temperature synthesis of ordered mesoporous silicas from solo hydrocarbon surfactants and understanding of their synthetic mechanisms. *J. Mater. Chem.* **2009**, *19* (5), 661–665.